

On the behaviour of the IR Ca II triplet in normal and active galaxies

Elena Terlevich,^{1,3} Angeles I. Díaz² and Roberto Terlevich³

¹ Astronomy Centre, Sussex University, Falmer, Brighton, BN1 9QH

² Dpto. de Física Teórica, C-XI, Universidad Autónoma de Madrid, 28049-Madrid, Spain

³ Royal Greenwich Observatory, Herstmonceux, BN27 1RP

Accepted 1989 June 23. Received 1989 June 20; in original form 1988 November 7

SUMMARY

Ca II triplet in absorption at $\lambda\lambda 8498, 8542, 8662 \text{ \AA}$ is the strongest feature in the infrared spectrum of late-type stars and normal galaxies. Its strength has been found to be a good luminosity indicator for metal-rich stellar populations. We present high signal-to-noise near-IR spectroscopic data for the nuclear region of 42 normal and active galaxies. We have explored the behaviour of the Ca II triplet strength and found that it shows a small spread around a mean value of 7 \AA for our sample of normal galaxies. We also found that, in all the Seyfert type 2 galaxies measured and even in some Seyfert type 1, while the optical stellar features show substantial dilution, the strength of the IR Ca II triplet is equal to and in some cases larger than that in normal elliptical galaxies. This result is most naturally explained by the presence of young stars dominating, or at least contributing heavily to, the unresolved nuclear light at near-IR wavelengths. These findings constitute strong evidence for a stellar population substantially younger than that observed in normal early-type galaxies and give support to the starburst scenario for nuclear activity.

The large equivalent width of the IR Ca II triplet in Seyfert nuclei provides a unique method of probing the gravitational potential close to the central engine. This method is relatively insensitive to the presence of ionized gas in the nuclear regions. Analysis with a cross-correlation technique has produced nuclear velocity dispersions accurate to ~ 10 per cent. We find that nuclear velocity dispersions in ‘active’ galaxies are comparable to those in normal ones of similar luminosity. We compare the width of the [O III] and [S III] forbidden lines with the stellar velocity dispersion and find that Seyfert type 2 galaxies and NGC 1052 show an additional broadening affecting the forbidden lines that is not seen in our starbursts or Seyfert type 1.

1 INTRODUCTION

It has become customary to divide galactic nuclei into two main groups: ‘normal’ and ‘active’, referring to nuclei whose properties can and cannot be explained in the context of normal star formation and evolution, respectively. However, a clear division between these two classes does not exist, and a continuity and/or overlap of properties between both has been reported in radio (Condon *et al.* 1982), IR (Rieke & Lebofsky 1979) and X-ray (Lawrence *et al.* 1985) surveys of luminous galaxies. In fact, the possibility of a connection between the presence of hot young stars and nuclear activity has been recognized by several authors (Pronik 1973; Adams & Weedman 1975; Harwit & Pacini 1975; Osterbrock 1978; Weedman 1983).

Traditionally, the ionizing source of the gaseous emission in Active Galactic Nuclei (AGN) is assumed to be non-

thermal in origin, and, in the case of Seyfert type 1 galaxies and quasars, is attributed to a hot accretion disc circling a central black hole (Rees 1984, and references therein). This mechanism has been further extrapolated to objects with a lower level of activity: Seyfert type 2 galaxies and LINERS (see e.g. Heckman 1987). However, Terlevich & Melnick (1985) have shown that for these latter objects the observed emission-line spectra can be equally well reproduced by Violent Star Formation (VSF) processes in a high-metallicity environment, such as the one expected in the nuclei of early-type galaxies (Pagel & Edmunds 1981; Phillips, Charles & Baldwin 1983; Phillips *et al.* 1984; Díaz, Pagel & Wilson 1985). Other observations generally accepted as evidence for the presence of a massive black hole in the centres of AGN, like broad permitted lines and variability, can also be explained by the same star formation processes (Terlevich, Melnick & Moles 1987; Terlevich & Melnick 1987, 1988;

Filippenko 1989). It is therefore obvious that just the analysis of the emission-line ratios of these galaxies, which has been the only criterion used in most cases to classify an object as an AGN, will not allow a distinction between the 'active' and 'non-active' hypotheses. Ways to discriminate between the two alternatives have to be found in other properties of their nuclear regions.

One of these properties is the blue featureless continuum detected in most, if not all, Seyfert galaxies and some LINERS. This continuum originates in an unresolved point-like nucleus identified with the ionizing central source and is well represented in the optical range by a power-law dependence of the flux density on frequency. Its contribution to the total nuclear light can be calculated for nearby galaxies (Yee 1983; Malkan & Filippenko 1983) and is found to be quite substantial in the case of Seyfert type 2 galaxies. In Seyfert galaxies of type 1 this unresolved component clearly dominates the light at visible wavelengths.

The detailed study of this continuum is in many cases difficult because of substantial contamination from stellar light,

but it can provide important clues about its physical origin. Its properties should be qualitatively different according to whether the continuum originates in an accretion disc or in a young cluster. In the classical non-thermal case the continuum should be featureless and bluer than the old population present in the bulges of spiral galaxies; therefore, all stellar absorption features should be weaker than in normal galaxies by an amount that is wavelength dependent. In the VSF scenario, however, the blue continuum would originate in a reddened young cluster; it should then be highly featureless in the blue (Kinman & Davidson 1981; Rayo, Peimbert & Torres-Peimbert 1982; Melnick, Moles & Terlevich 1985), since the optical spectra of the OB stars responsible for the optical continuum show very weak or absent absorption lines in the $\lambda\lambda 3500-7500$ Å spectral region. The near-IR Ca II triplet ($\lambda\lambda 8498, 8542, 8662$ Å), however, is very sensitive to luminosity, its strength increasing with decreasing stellar surface gravity (Jones, Alloin & Jones 1984; Díaz, Terlevich & Terlevich 1989, hereafter DTT89) and should be strong if the star cluster is old enough to contain some luminous red

Table 1. Galaxy parameters.

Name	Morph	T	NT	Ref	B_T	Ref	M_{BT}	M_{bulge}	Σ	Code	
N221	M32	E2	-6	5	*	8.79	SA	-15.53	-15.53	9.8	1
N224	M31	Sb	3	5	*	2.71	SA	-21.61	-19.99	13.4	2
N262	Mk348	S0/a	0	2	K78	*	*	*	*	*	3
N598	M33	Sc(s)	6	5	*	5.69	SA	-19.07	-15.64	*	3
N821	*	E6	-5	5	*	11.89	SA	-21.01	-21.01	13.0	1
N1023	*	SB0	-3	5	*	10.09	SA	-21.17	-20.50	12.0	1
N1052	*	E3/S0	-5	3	H80	11.53	SA	-20.90	-20.90	12.0	4
N1068	*	Sb(rs)	3	2	K78	9.03	SA	-22.93	-21.31	11.0	5
	III Zw55	*	* 2	K78	*	*	*	*	*	*	3
	IC342	Scd	5	5	*	9.12	RC2	*	*	*	6
N1667	*	Sc	5	2	VV85	*	SA	-22.54	-20.02	12.2	1
N1700	*	E3	-5	5	*	11.81	SA	-22.67	-22.67	12.1	1
	Mk3	S0	-2	2	K78	*	*	*	*	*	6
	Mk78	*	* 2	K78	*	*	*	*	*	*	3
N2685	Arp336	S0p	-2	5	*	11.86	SA	-19.65	-19.05	13.0	1
N2693	*	E2	-5	5	*	12.70	SA	-22.32	-22.32	12.8	1
N2782	*	Sa(s)p	1	4	VV85	11.50	SA	-22.06	-20.93	12.6	1
N2911	*	S0p	-2	3	H80	12.53	SA	-21.36	-20.76	13.9	3
N2992	*	Sa	1	2	*	11.61	SA	-21.36	-20.23	*	3
N3031	M81	Sb(r)	2	3	H80	7.01	SA	-20.75	-19.53	12.5	7
N3227	*	Sb(s)	3	1	VV85	10.92	SA	-20.80	-19.18	13.0	7
N3310	*	Sbc(r)p	5	4	VV85	10.84	SA	-20.82	-18.30	9.7	8
N3393	*	*	* 2	VV85	*	*	*	*	*	*	8
N3504	*	Sb(s)	3	4	VV85	11.25	SA	-21.11	-19.49	11.8	8
N3516	*	RSB0	-2	1	VV85	12.34	SA	-21.43	-20.83	10.4	8
N3642	*	Sb(r)	4	3	H80	11.01	SA	-21.69	-19.84	*	3
	Mk176	*	-2	2	K78	*	*	*	*	*	9
N4151	*	Sab	2	1	VV85	10.53	SA	-20.93	-19.71	12.1	8
N4258	M106	Sb(s)	4	3	H80	8.04	SA	-22.05	-20.20	13.2	8
N4278	*	E1	-5	3	H80	11.13	SA	-19.24	-19.24	11.6	8
N4388	*	Sab	3	2	VV85	10.65	SA	-21.05	-19.43	*	9
N4472	M49	E1/S0	-3	5	*	9.32	SA	-22.38	-21.81	12.4	3
N4725	*	Sb/SB(r)	3	5	*	9.37	SA	-22.47	-20.85	*	8
N4736	M94	RSab(s)	2	3	H80	8.38	SA	-20.81	-19.59	10.3	8
N5347	*	SB(s)	2	2	VV85	12.86	SA	-20.54	-19.32	*	8
N5866	M102	S0	-2	5	*	10.86	SA	-20.22	-19.62	11.4	8
N5953	*	*	1	2	VV85	*	*	*	*	*	8
N6217	*	RSBbc(s)	5	4	*	11.41	SA	-21.11	-18.59	12.6	8
N6340	*	Sa(r)	1	5	*	11.29	SA	-21.05	-19.92	13.0	8
N6384	*	Sb(r)	3	5	*	10.42	SA	-22.28	-20.66	13.8	8
N6500	*	Sab	2	3	VV85	*	*	*	*	*	4
N7479	*	SBbc(s)	5	3	*	11.27	SA	-22.34	-19.82	13.4	7

References

- K78: Keel 1978
H80: Heckman 1980
VV85: Véron-Cetty & Véron 1985
SA: Sandage & Tammann 1981
RC2: de Vaucouleurs *et al.* 1976

supergiants, since these stars dominate the near-IR light. Therefore, although the optical absorption lines should be diluted with respect to normal galaxies, little or no dilution should be observed in the IR Ca II triplet.

We have explored the behaviour of the IR Ca II triplet both in normal and active galaxies in order to investigate the possible effects of dilution in these lines and to try to shed some light on the nature of the ionizing source in AGN. Section 2 of this work presents the observations and the reductions. Section 3 describes the methods employed in the analysis of the data and Section 4 is devoted to the presentation of the results and their discussion.

2 OBSERVATIONS AND REDUCTIONS

Spectra of 42 galaxies, as well as stars, were obtained in four different observing runs in 1984 August and December, 1986 November and 1987 May with the INT at the Roque de los Muchachos Observatory on the Spanish island of La Palma using the Intermediate Dispersion Spectrograph (IDS), the 235- and 500-mm cameras and a CCD detector with a GEC-type P8600 front-illuminated chip.

The stars embrace a wide range of surface gravities and metallicities, providing a good stellar reference frame in the same system as the galaxies. The galaxy observations will be described here, while those concerning the stars are described elsewhere (DTT89).

Table 1 gives the main characteristics of the galaxies observed: name, morphological type and T as given in the *Second Reference Catalogue of Bright Galaxies* (de Vaucouleurs, de Vaucouleurs & Corwin 1976), the nuclear type defined as follows: 1 = Seyfert type 1; 2 = Seyfert type 2; 3 = LINER; 4 = starburst nucleus* and 5 = normal nucleus and a reference for the nuclear type. Also given in the table are the apparent blue magnitude (B_T) and the absolute blue magnitude (M_{B_T}), taken from the *Revised Shapley-Ames Catalog of Bright Galaxies* (Sandage & Tammann 1981) except when stated otherwise; the bulge magnitude M_{bulge} derived from Simiens & de Vaucouleurs (1986), surface brightness (Σ) and a code to indicate the instrumental configuration used (see Table 2).

The galaxy spectra taken during the first two runs were obtained as part of a wider programme designed to observe the [S III] emission lines at $\lambda\lambda 9069, 9532 \text{ \AA}$ in AGN and cover the wavelength range $\sim \lambda\lambda 8500 - 9900 \text{ \AA}$. With this set up, the IR Ca II triplet lies at the blue edge of the spectra. The rest of the observations were made specifically for this study and therefore cover more suitable wavelength ranges ($\lambda\lambda 7900 - 9300 \text{ \AA}$ for the 235-mm camera and $\lambda\lambda 7400 - 9100 \text{ \AA}$ for the 500-mm one). For the observations made with the 235-mm camera we used a 400 g mm^{-1} grating providing a dispersion of 104 \AA mm^{-1} at 8500 \AA which, with the slit width used for the observations ($180 - 360 \mu\text{m}$), yielded a spectral resolution of $3 - 5 \text{ \AA}$ approximately. For the 500-mm camera we used a 150 g mm^{-1} grating providing a dispersion of $131.2 \text{ \AA mm}^{-1}$ at $\lambda 8500 \text{ \AA}$. The slit width used was always $\sim 180 \mu\text{m}$ giving a spectral resolution of about 9 \AA . The size of the CCD along the spatial direction is 400

Table 2. Journal of observations.

Date	Camera	λ range (\AA)	Dispersion (\AA/mm)	Proj. slit (\AA)	Slit width (μm)	Code
18/19 Aug. 84	235mm	6287-9813	104.4	3	185	4
19/20 Aug. 84	235mm	7915-9243	104.4	2	80	2
19/20 Aug. 84	235mm	6287-9813	104.4	3	185	4
20/21 Aug. 84	235mm	6287-9813	104.4	5	270	7
19/20 Dec. 84	235mm	6187-9813	104.4	5	270	7
19/20 Dec. 84	235mm	8487-9813	104.4	5	270	6
20/21 Dec. 84	235mm	8487-9813	104.4	4	210	3
21/22 Dec. 84	235mm	6187-9813	104.4	4	210	5
21/22 Dec. 84	235mm	8487-9813	104.4	4	210	3
21/22 Dec. 84	235mm	8487-9813	104.4	7	360	9
24/25 Nov. 86	500mm	7425-9091	131.2	9	185	1
25/26 Nov. 86	500mm	7425-9091	131.2	9	185	1
26/27 Nov. 86	500mm	7425-9091	131.2	9	185	1
15/16 May 87	235mm	7931-9257	104.4	5	300	8
16/17 May 87	235mm	7931-9257	104.4	5	300	8
16/17 May 87	235mm	7931-9257	104.4	5	300	8
18/19 May 87	235mm	7931-9257	104.4	5	300	8

pixels of 0.7 arcsec in the case of the 235-mm camera and 0.4 arcsec if using the 500-mm one. A journal of observations is given in Table 2.

The reduction of the data was carried out at the STARLINK node in RGO using standard software packages. The procedure included subtraction of a dark current bias and pre-flash frames, as well as the removal of cosmic rays due to the long exposure times involved (about 2000 s). The data were subsequently divided by a flat field and wavelength calibrated. A number of pixels were added for the extraction of one-dimensional spectra, according to the seeing conditions during the observations. The slit length was 2.4 arcmin and covered the object as well as a substantial part of the sky that was used for background subtraction. The atmospheric bands (mainly water vapour) present in the spectra (see Díaz, Pagel & Wilson 1985) do not affect the Ca II triplet and therefore were not removed. No flux calibration was performed. Reduced spectra for representative galaxies of every nuclear type are shown in Fig. 1(a), (b), (c), (d) and (e). The spectra shown in Fig. 1(f) have been obtained using instrumental configuration 3 and the Ca II triplet lies at the edge of the spectra.

3 METHODS OF MEASUREMENT

Absolute results for any equivalent width depend to some extent on how the measurement is made. To derive useful information from equivalent width studies requires comparison between values corresponding to different objects. It is therefore important to define clearly the system in which the measurements are made, so that they can be used in other studies. In what follows we describe the method we have employed.

The strengths of the three Ca II lines were measured for all the objects in the sample with respect to a pseudo-continuum defined using chosen side-bands. As we shall see below, the positions of these side-bands represent the best compromise for accurate measurements of the strength of the Ca II lines. The width of the spectral region corresponding to each line was selected to minimize the effect of 'smearing' due to the different broadenings of the lines in the galaxies of our sample. The pseudo-continuum was defined by a linear fit to the mean fluxes in the chosen side-bands.

We find that the continuum is remarkably flat in F_λ

* Starburst nuclei do not include late-type spirals undergoing normal star formation. These latter galaxies are considered as normal for their morphological type.

between $\lambda 8440 \text{ \AA}$ and $\lambda 8800 \text{ \AA}$, both for our sample of galaxies and for a large catalogue of stellar spectra (DTT89) covering a wide range of effective temperature, surface gravity and metallicity. Therefore we chose the side-bands centred at 8455 \AA and 8850 \AA with a width of 15 \AA (Fig. 2). This continuum choice has the advantage of defining a Ca II strength measure which is essentially free of any TiO contribution (see Fig. 2). Four of the galaxies (NGC 3642, NGC 4472, Mk 176 and IC 342) observed in 1984 have the Ca II triplet close to the blue edge of the spectrum; an optional continuum band at $\lambda 8582 \text{ \AA}$ had to be used. This continuum placement was also used for the Seyferts type 1 showing broad O I $\lambda 8440 \text{ \AA}$ emission.

Line boundaries were taken at 15 \AA each side of every line centre and a pseudo-equivalent width was computed by adding the flux inside the line boundaries below the pseudo-continuum and dividing by the corresponding value of the continuum:

$$W_{\lambda_c} = \left(1 - \frac{\text{Total flux}(\lambda_c - \Delta\lambda, \lambda_c + \Delta\lambda)}{\text{monochromatic flux pseudo continuum}(\lambda_c)} \right) * 2\Delta\lambda.$$

In what follows we shall call it equivalent width (EW) for simplicity.

To estimate the systematic differences affecting the EW determined by using the optional blue side-band we measured the sample of normal galaxies in both systems and found that the EW(Ca II) measured with the optional side-band is on average 15 per cent smaller. A correction was accordingly included in the measurements.

An additional problem for the measurement of equivalent widths in galaxies is related to their internal velocity dispersions and the corresponding broadening of the spectral lines which affect both the continuum level and the lines themselves. A correction has to be applied, therefore, to compare measurements both of galaxies with different velocity dispersions and of galaxies with stars. To accomplish this, spectra of representative stars were smoothed by convolution with Gaussians of different widths so as to mimic velocity dispersions of up to 500 km s^{-1} and EWs of the Ca II lines were measured for each smoothed spectrum. Stars with different spectral types give similar results within an rms scatter of about 0.1 \AA . Fig. 3 shows the relationship between σ (disper-

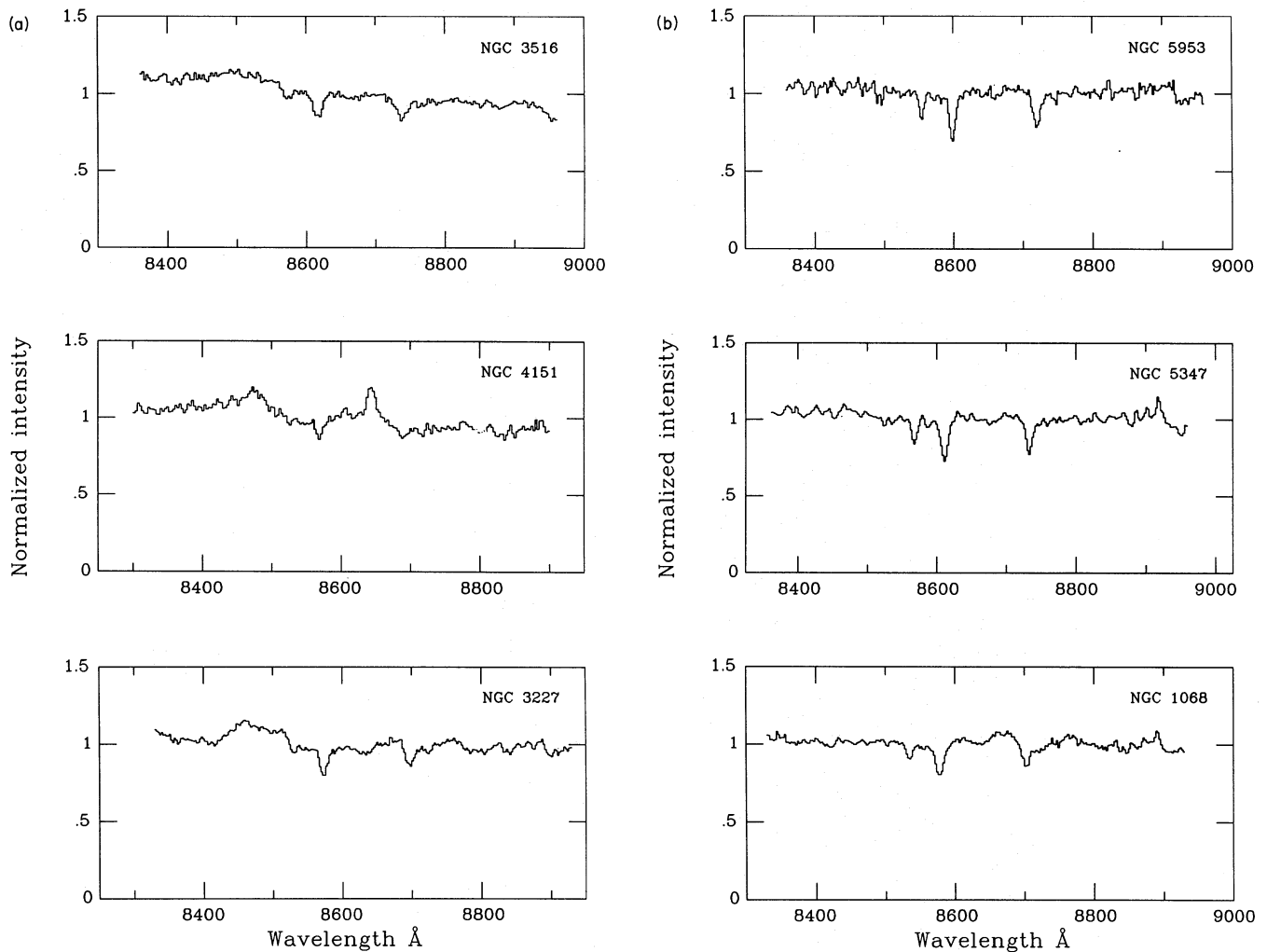


Figure 1. Reduced normalized spectra for representative galaxies of every nuclear type: (a) Seyfert type 1; (b) Seyfert type 2; (c) LINER; (d) Starburst; (e) Normal and (f) with instrumental configuration 3 that leaves the Ca II triplet at the edge of the spectra.

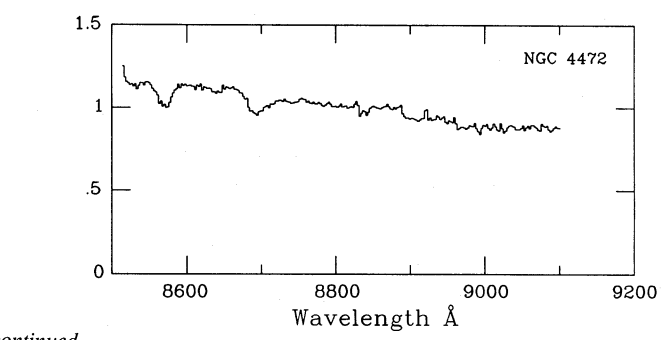
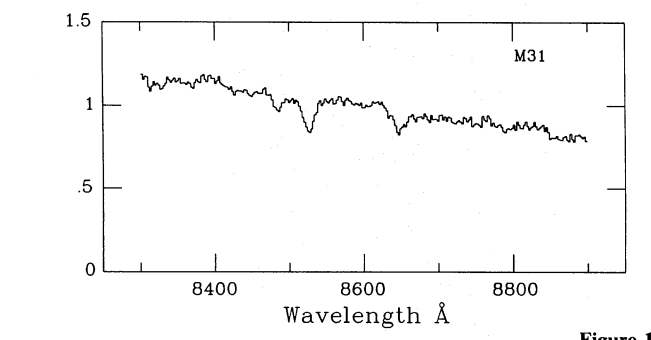
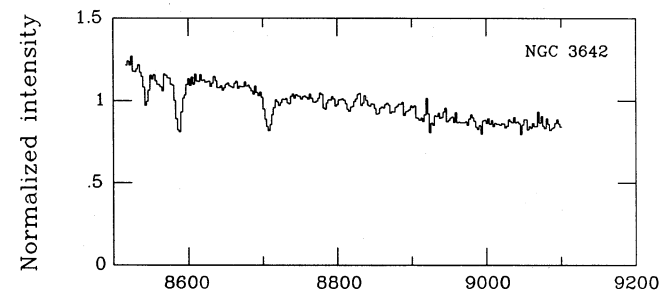
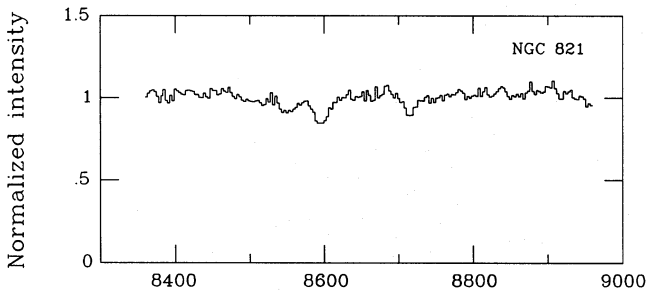
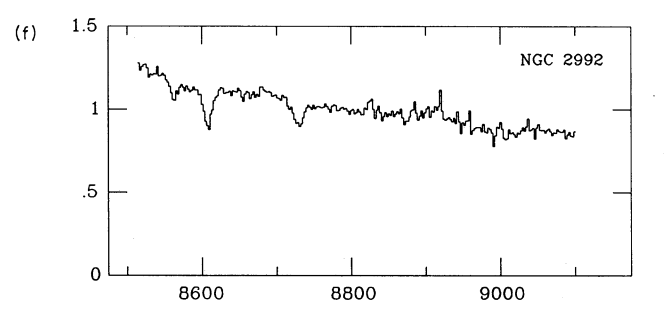
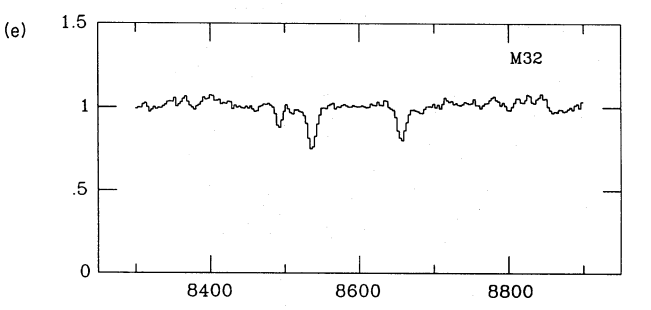
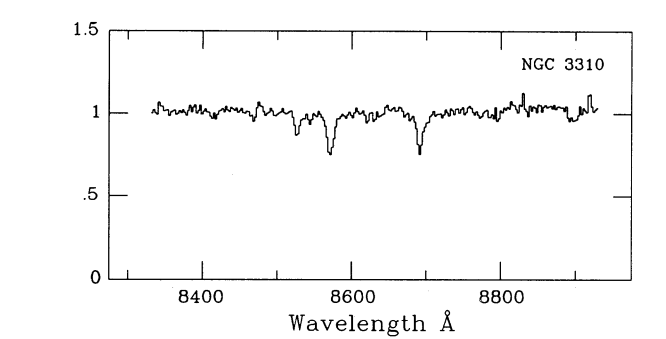
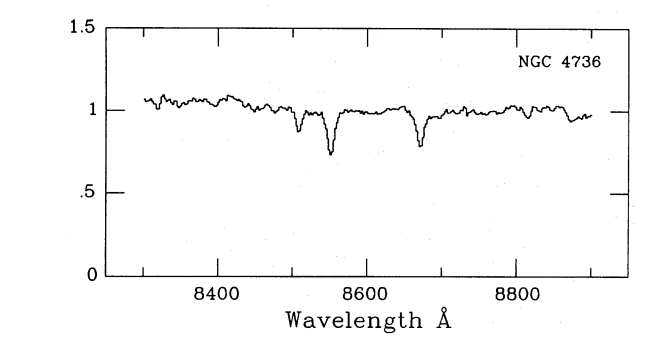
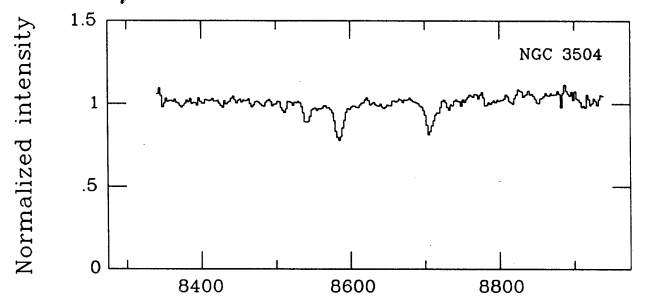
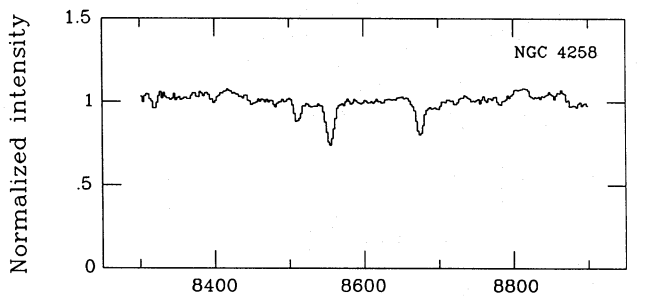
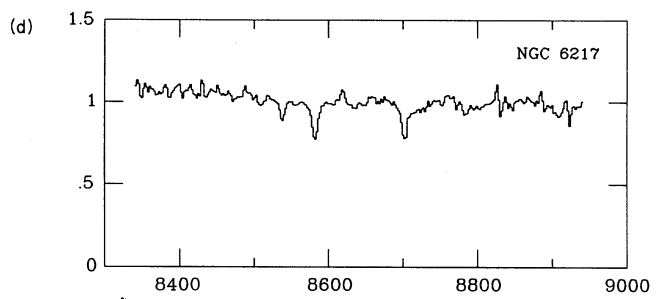
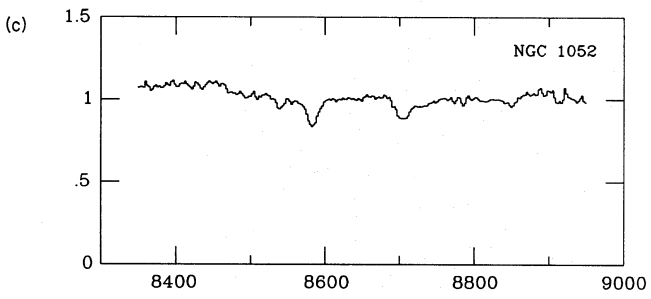


Figure 1 - continued

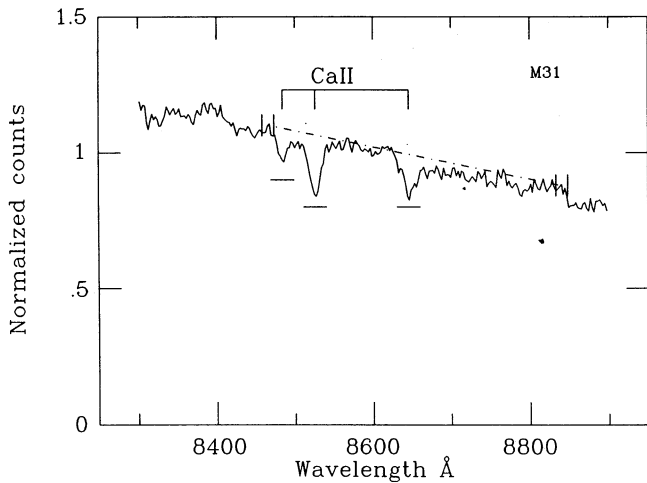


Figure 2. Continuum, line windows and side-bands used to measure $\text{EW}(\text{Ca II})$.

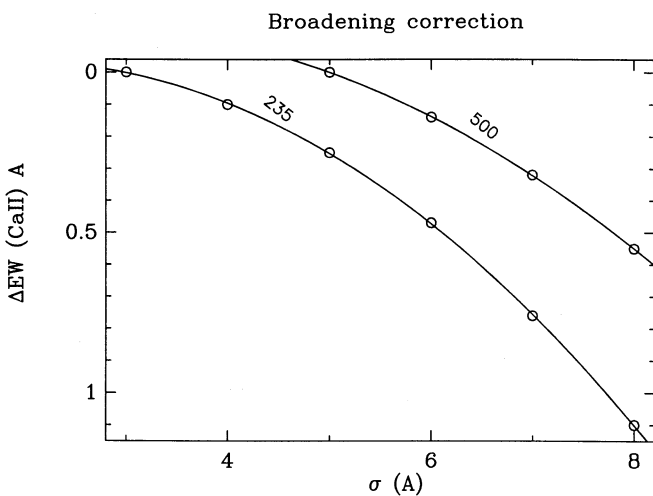


Figure 3. Broadening correction curves for the 235- and 500-mm cameras. σ_{sp} (Å) is the dispersion of the convolution of different Gaussians with a stellar spectrum, and $\Delta\text{EW}(\text{Ca II})$ is the difference in the measurements of the EW of the Ca II triplet two strongest lines added together, for the stellar spectra without and with broadening.

sion in Å of the Gaussian) and the mean equivalent width correction [$\Delta\text{EW}(\text{Ca II})$] given by the average difference between the measures of the two strongest spectral lines of Ca II without and with broadening. A least-squares fitting gives

$$\Delta\text{EW}(\text{Ca II}) = 0.032\sigma_{\text{sp}}^2 - 0.133(\sigma_{\text{sp}}) + 0.12 \quad \sigma_{\text{sp}} > 3 \text{ \AA},$$

for the 235-mm camera and

$$\Delta\text{EW}(\text{Ca II}) = 0.032\sigma_{\text{sp}}^2 - 0.243(\sigma_{\text{sp}}) + 0.44 \quad \sigma_{\text{sp}} > 5 \text{ \AA},$$

for the 500-mm camera. σ_{sp} is the observed spectral rms width in Å and includes the instrumental resolution. A reasonable approximation is $\sigma_{\text{sp}}^2 = \sigma_*^2 + A^2$ where A is 3 Å for the 235-mm and 5 Å for the 500-mm cameras.

The effect of the broadening is to decrease the measured EWs. We have referred our measurements to zero velocity dispersion values (instrumental broadening); this has the

additional advantage of allowing a direct comparison with a stellar reference system. The 1984 observations, not made specifically for this project, range in spectral resolution from 2.5 to 3.3 Å. The broadening correction for all of them is inside the errors, nevertheless, the same as that for our main set-up (3.0 Å resolution for code 8 in Table 2), so we used the same correction curve for all the observations with the 235-mm camera. The broadening correction, calculated according to the expressions above using the value of the σ_{sp} determined for each spectrum, was added to the measured $\text{EW}(\text{Ca II})$. For the eight galaxies observed with the 500-mm camera, there is an additional zero-point correction of 0.2 Å, to compensate for the different resolution.

The velocity dispersions were obtained using the cross-correlation method (Tonry & Davies 1979), which requires the comparison of a stellar template with the spectrum of each galaxy. The velocity dispersion is derived from the width of the cross-correlation function after deconvolution with the instrumental profile. At any rate, as pointed out by Dressler (1984) and Davies *et al.* (1987), the measured systemic velocity and σ are independent of the method used. Nominal errors, not including systematic ones, are $\leq 50 \text{ km s}^{-1}$ for the systemic velocity and ≤ 10 per cent for σ .

The results of the measurements are given in Table 3. This table gives for each galaxy the redshift $1+z$ (as obtained from the cross-correlation) the velocity dispersion in km s^{-1} corrected for instrumental broadening, the measured equivalent width in Å for each of the Ca II triplet lines, the broadening correction in Å for the two strongest lines ($\lambda\lambda 8542, 8662 \text{ \AA}$), the corrected value of these two lines added together and the value in arcsec corresponding to each extraction.

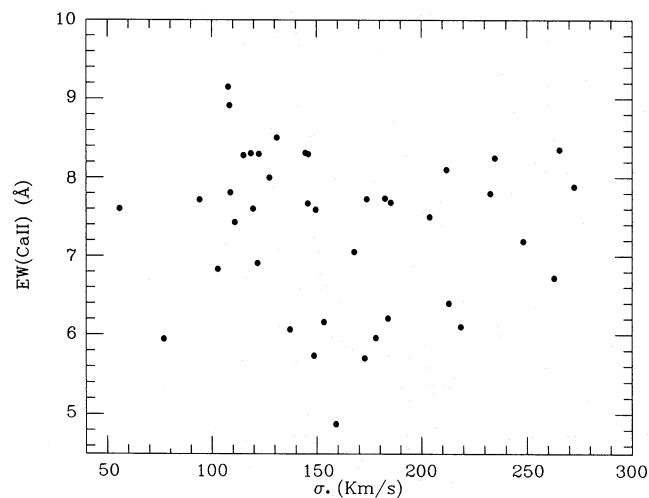
Other methods have been used in previous studies of the Ca II triplet (Cohen 1978, 1979; Jones, Alloin & Jones 1984; Carter, Visvanathan & Pickles 1986); ours nevertheless offers two main advantages over them: the measure of the Ca II triplet strength is not affected by the presence of TiO bands and the method allows a direct comparison with a stellar reference system. Due to their different choice of continuum fitting, the values of Jones, Alloin & Jones (1984) included a contribution from TiO which was substantial for the coolest M stars. Carter, Visvanathan & Pickles' (1986) measurements do not suffer from this problem but they chose to smooth their stellar spectra to match the typical galaxy resolution, thus defining an *ad hoc* system. Our measurements also include a correction due to the different velocity dispersions in the galaxy spectra which is not included in Cohen's (1978, 1979) measurements, even though she recognized the importance of the effect. The inclusion of this broadening correction does not introduce any systematic effect; this can be seen in Fig. 4 where we have plotted the corrected $\text{EW}(\text{Ca II})$ versus the stellar velocity dispersion.

The error in our measurements has been estimated quantitatively following the error analysis of spectroscopic features by Rich (1988). For a typical spectrum, the number of counts per pixel in the continuum is about 10^3 or 10^4 . The estimation of the rms error in the Ca II strengths due solely to photon statistics is 0.1 Å. It is therefore obvious that this cannot be the main source of error in our data. It should also be remembered that two different instrumental configurations and two different GEC chips were used during the

Table 3. Measured quantities for the Galaxy sample.

Name	$1+z$	Ca1 (Å)	Ca2 (Å)	Ca3 (Å)	$\Delta EW(CaII)$ (Å)	$EW(CaII)$ (Å)	σ_* (km s^{-1})	Extraction (")
M32	0.9995	1.5	3.8	3.6	0.2	7.6	56	1.6
M31	0.9983	1.3	3.3	2.5	0.2	6.1	137	1.2
Mk348	1.0160	2.8	4.6	2.6	0.5	7.7	185	2.8
M33	0.9994	—	3.3	3.5	0.1	6.9	77	2.8
N821	1.0062	1.8	3.4	2.4	0.6	6.4	213	2.4
N1023	1.0023	1.5	3.6	3.4	0.6	7.5	204	4.0
N1052	1.0047	1.4	3.7	3.5	1.1	8.3	265	3.5
N1068	1.0043	1.7	3.6	2.2	0.3	6.2	153	2.8
IIIZw55	1.0257	1.9	4.2	3.2	0.7	8.1	212	2.8
IC342	1.0000	—	2.9	3.0	0.1	5.9	77	2.8
N1667	1.0153	1.1	3.1	2.2	0.5	5.7	173	1.6
N1700	1.0129	1.2	3.2	2.2	0.6	6.1	219	2.4
Mk3	1.0136	1.9	3.9	2.3	1.0	7.2	248	2.8
Mk78	1.0370	2.0	3.6	4.6	0.2	8.3	115	2.8
N2685	1.0023	1.8	3.9	4.1	0.3	8.3	122	2.8
N2693	1.0164	2.4	4.0	2.7	0.2	6.8	*	2.8
N2782	1.0215	2.2	3.8	4.1	0.4	8.3	146	2.4
N2911	1.0092	1.7	4.0	3.0	0.8	7.8	233	2.8
N2992	1.0079	2.0:	4.9	4.1	0.1	9.1	108	5.6
M81	1.0003	1.7	4.2	3.1	0.4	7.7	174	2.8
N3227	1.0038	—	2.8	1.7	0.3	4.9	159	2.1
N3310	1.0035	2.0	3.7	3.6	0.2	7.4	111	4.2
N3393	1.0126	0.3	2.8	2.9	0.5	6.2	184	2.1
N3504	1.0054	1.9	3.8	3.6	0.2	7.6	120	6.3
N3516	1.0088	1.8	3.8	3.5	0.9	8.2	235	2.1
N3642	1.0052	2.1	4.1	3.6	0.1	7.8	109	5.6
Mk176	1.0082	1.6	1.7	3.7	0.3	5.7	148	2.8
N4151	1.0032	1.6	2.9	2.6	0.5	6.0	178	2.1
N4258	1.0016	1.6	3.9	3.4	0.3	7.7	146	4.9
N4278	1.0024	1.4	3.6	3.0	1.3	7.9	272	4.2
N4388	1.0087	1.9	4.3	3.9	0.2	8.3	119	2.8
N4472	1.0036	—	2.8	2.8	1.1	6.7	263	5.6
N4725	1.0040	1.8	4.2	3.8	0.3	8.3	145	3.5
N4736	1.0011	1.8	3.9	3.4	0.3	7.6	150	2.1
N5347	1.0081	1.4	3.5	3.2	0.1	6.8	103	5.6
N5866	1.0025	1.8	3.8	3.4	0.5	7.7	183	2.8
N5953	1.0067	1.9	4.1	3.5	0.1	7.7	94	2.1
N6217	1.0048	2.6	4.0	4.3	0.2	8.5	131	3.5
N6340	1.0041	1.9	4.2	3.5	0.2	8.0	127	4.9
N6384	1.0056	1.7	3.8	2.9	0.2	6.9	122	3.5
N6500	1.0102	1.6	3.5	3.1	0.4	7.0	168	2.8
N7479	1.0078	3.1	5.0	3.8	0.1	8.9	109	4.9

*Unresolved

**Figure 4.** Broadening corrected $EW(CaII)$ (Å) versus the stellar velocity dispersion σ_* (km s^{-1}) for the sample's galaxies.

whole observing programme and that might introduce external errors. A more realistic estimate of the errors would need repeated observations of the same object; unfortunately we did not perform enough repeated observations. A more

practical approach, though not so satisfactory, is to estimate an upper limit to the errors by assuming that all the 13 normal galaxies in our sample have the same intrinsic strength and therefore the rms of the sample represents this upper limit. We thus take 0.80 \AA to be our average error of measurement.

4 DISCUSSION

4.1 Ca II strength

Fig. 5 shows the distribution of the strength of the Ca II lines ($\lambda\lambda 8542, 8662 \text{ \AA}$) versus galactic nuclear type as given in Table 1. Other absorption lines besides the Ca II triplet appear in the same spectral region (e.g. Fe I $\lambda\lambda 8387, 8515, 8687 \text{ \AA}$) and in particular the Fe I line at $\lambda 8687 \text{ \AA}$ in the red wing of Ca II $\lambda 8662 \text{ \AA}$ and a Fe I blend close to its blue wing, which vary from galaxy to galaxy. Our results, however, seem to be free of contamination by these lines, since essentially the same relationship between $EW(CaII)$ and nuclear type is obtained using only the $\lambda 8542 \text{ \AA}$ line. The weakest $\lambda 8498 \text{ \AA}$ line lies on the very edge of the spectrum for some galaxies of the sample (see Section 2). We have therefore not used this line in our analysis. In fact, given the larger error of this line,

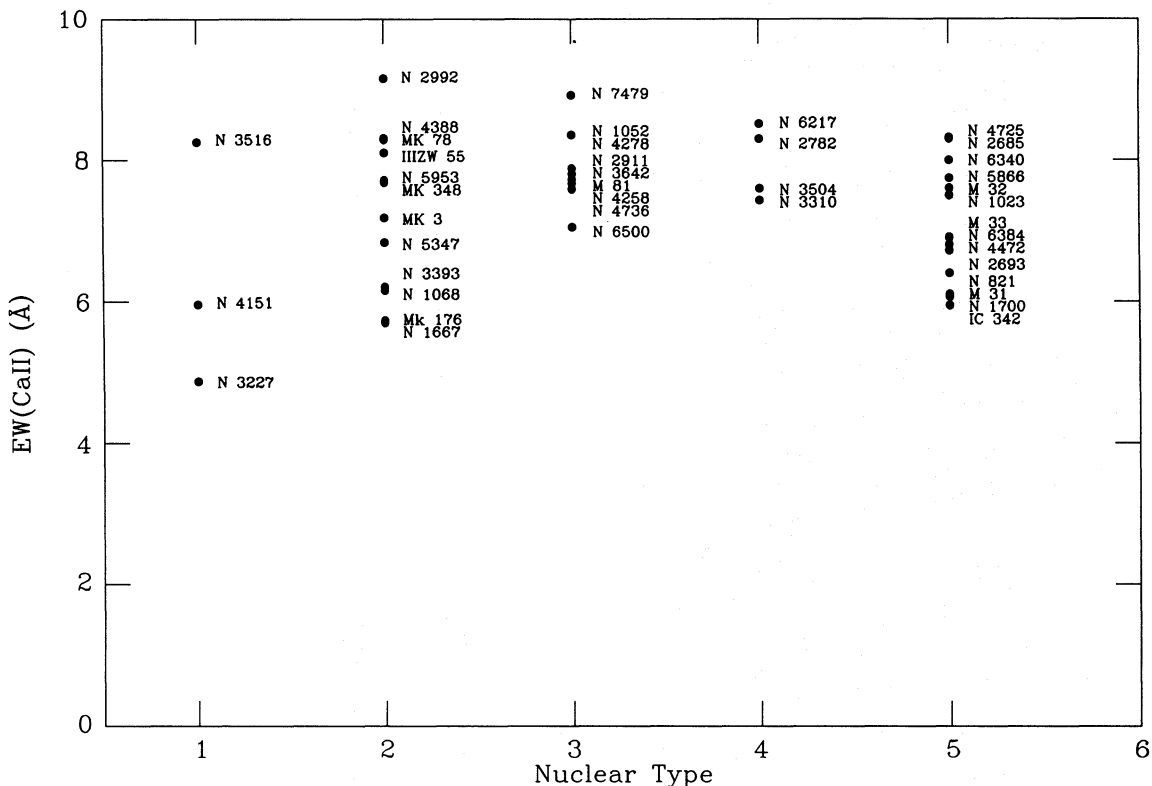


Figure 5. Broadening corrected strength of the two more intense Ca II triplet lines ($\lambda\lambda 8542, 8662 \text{ \AA}$) added together, as a function of nuclear type as given in Table 1, 1: Seyfert 1; 2: Seyfert 2; 3: LINER; 4: Starburst; 5: Normal. Average rms error is 0.8 \AA .

its addition not only does not improve the signal-to-noise ratio of the measurement, but in some cases slightly decreases it.

It can be seen from Fig. 5 that normal galaxies have a remarkably small spread in $EW(\text{Ca II})$, about 10 per cent with mean value 7.1 \AA . Even considering the range in velocity dispersion, galaxy type and luminosities of the galaxies involved, this result is not unexpected. DTT89 have shown, from the analysis of the $EW(\text{Ca II})$ in galactic stars, that for abundances above $1/2$ solar the $EW(\text{Ca II})$ is an excellent gravity indicator with no metallicity dependence. Thus the observed mean value and small scatter in normal galaxies is a clear confirmation that the nuclear light is dominated by red giants. Among the normal galaxies not undergoing star formation (all except IC 342) there seems to be a certain tendency for elliptical galaxies to show smaller values of $EW(\text{Ca II})$ than spirals. This trend should be further explored with a larger sample. Fig. 5 also shows that most Seyfert 2 galaxies and LINERS have equivalent widths of the Ca II lines which are similar to, or even stronger than, those corresponding to normal galaxies (nuclear type 5); starburst galaxies show Ca II lines similar to those of normal galaxies of the same morphological type. We are analysing a larger sample of nuclei with H II region type spectra (starburst galaxies and late-type spirals) in order to investigate the effects of star formation on the Ca II triplet (Terlevich, Terlevich & Díaz, in preparation). There are only three Seyfert type 1 galaxies in our sample: NGC 3227, NGC 3516 and NGC 4151 and they show a large range of $EW(\text{Ca II})$. The IR Ca II lines have also been observed in a large sample of Seyfert 1 galaxies by Morris & Ward (1988) for a fraction

of which they quote values for the $\lambda 8542 \text{ \AA}$ line equivalent width between 1.1 and 4.6 \AA . These values, however, have to be taken with great caution due to the low resolution of their data, and they cannot be directly compared with ours since no information on their method of measurement is given.

The fact that the stellar absorption lines in the blue–yellow part of the spectrum appear substantially weakened in Seyfert galaxies as compared with normal ones seems to be well established. This weakening of the stellar lines implies the presence of an extra component of the continuum. This has usually been assumed to come from the nuclear ionizing source and to be of non-thermal origin. Equivalent widths of the Mg Ib line at $\lambda 5175 \text{ \AA}$ have been measured for a substantial number of Seyfert galaxies and LINERS (see the compilation by Dahari & De Robertis 1988) which can be compared with the average value measured for the nuclei of normal spiral galaxies (5.18 ± 0.71 ; Keel 1983). From the dilution thus computed and keeping the assumptions mentioned above, it is possible to predict the corresponding dilution that the IR Ca II lines should present.

A dilution factor for an absorption feature in the spectrum of any active galaxy can be defined as

$$D = \frac{EW_{\text{obs}}}{EW_{\text{ref}}},$$

where EW_{obs} is the equivalent width of the feature and EW_{ref} is the average equivalent width measured for normal spirals. Under the assumption of two components for the con-

tinuum, stellar and non-thermal, this factor can be written as

$$D^{-1} = 1 + \frac{I_{nt}}{I_g},$$

where I_{nt} and I_g represent the intensities of the non-thermal and stellar components of the continuum, respectively, at the central wavelength of the feature. The intensity of the non-thermal continuum can be represented by a power law of the form

$$I_{nt} \propto \lambda^{-\gamma}$$

and the continuum coming from an old stellar population is approximately flat per unit wavelength between 5000 and 10 000 Å (see for example Bica & Alloin 1987). Therefore the relation between the dilution factors at optical (5000 Å) and IR (8500 Å) wavelengths, D_{opt} and D_{IR} , respectively, can be written as

$$D_{IR}^{-1} = (1 - K^{-\gamma}) + K^{-\gamma} D_{opt}^{-1},$$

where $K = 8500/5000$ is the ratio of IR to optical wavelengths.

We have computed the IR dilution factors for the galaxies in our sample from their measured $EW(CaII)$ using as reference the normal early spiral mean value [$EW(CaII)_{ref} = 7.7 \pm 0.5$]. We have also computed optical dilution factors for those galaxies of the sample for which measurements of the equivalent width of the MgIb line $\lambda 5171$ Å exist (Dahari & De Robertis 1988). Both sets of values are given in Table 4. Fig. 6 shows these values together with the expected relation between the optical and IR dilution factors for different values of γ . The line with $\gamma = 0.5$ represents the canonical power law assumed for Seyfert type 2 galaxies ($F_\nu \propto \nu^{-1.5}$). All the Seyfert galaxies in this figure lie above that line and, in fact, above any line computed with other sensible value of γ . Although it is true

Table 4. Optical and infrared dilution.

Galaxy	$\frac{EW(MgI)_{obs}}{EW(MgI)_{ref}}$	$\frac{EW(CaII)_{obs}}{EW(CaII)_{ref}}$
Mk 348	0.42 ± 0.10	0.99 ± 0.16
NGC 1052	1.16 ± 0.28	1.10 ± 0.18
III Zw 55	0.43 ± 0.10	1.07 ± 0.17
Mk 3	0.79 ± 0.19	0.94 ± 0.15
Mk 78	0.25 ± 0.06	1.10 ± 0.18
NGC 3227	0.10 ± 0.02	0.63 ± 0.10
NGC 3393	0.46 ± 0.11	0.81 ± 0.13
NGC 3516	0.23 ± 0.06	1.08 ± 0.17
NGC 4388	0.83 ± 0.20	1.10 ± 0.18

that we are combining observations with different apertures for determining the dilution factors of MgIb and Ca II triplet, the IR apertures are the smaller ones. If the MgIb were observed through similar apertures, its dilution would presumably be even larger, making our conclusion stronger.

The fact that the Ca II triplet lines are seen at least at full strength in Seyfert galaxies, while other lines in the blue–yellow part of the spectrum appear substantially weakened as compared to normal galaxies, implies that the optical to IR continuum of Seyfert galaxies cannot be represented by a simple combination of an old stellar population and a featureless power-law continuum, unless that stellar population has Ca II triplet lines which are much stronger than those in normal elliptical galaxies.

The behaviour of the Ca II triplet in stars and globular clusters has been recently studied by different authors (Jones, Alloin & Jones 1984; Bica & Alloin 1987; Armandroff & Zinn 1988; DTT89). Although the Ca II triplet shows a biparametrical behaviour with surface gravity and metal abundance – the strength of the feature increasing with decreasing gravity and increasing abundance – at high

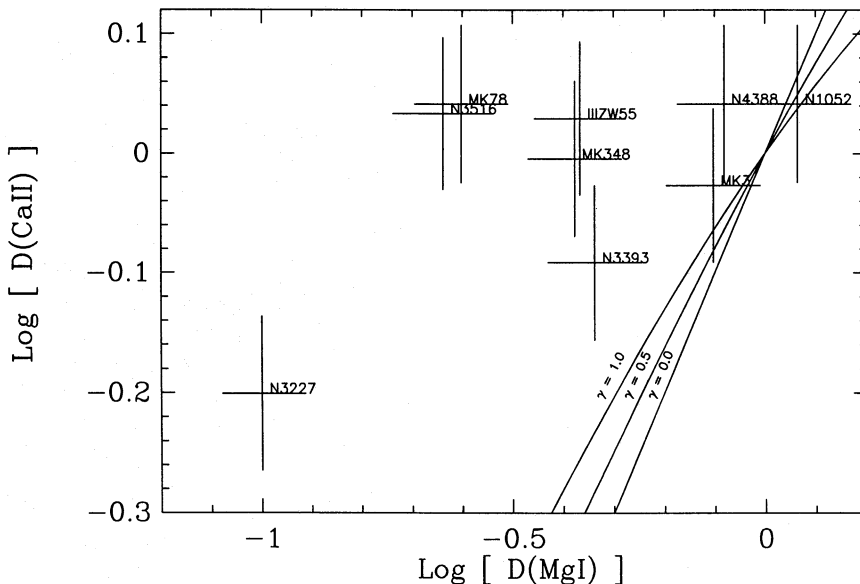


Figure 6. Dilution of the MgIb line ($\lambda 5171$ Å) versus the dilution of the Ca II lines ($\lambda \lambda 8542, 8662$ Å). The solid lines represent the expected relation between the dilutions in the optical and IR for different values of γ . The line with $\gamma = 0.5$ represents the canonical power law assumed for Seyfert 2 galaxies ($F_\nu \propto \nu^{-1.5}$).

metallicities the surface gravity becomes the dominant parameter. In fact, values of $EW(\text{Ca II})$ greater than 9 \AA are found only in red supergiant stars ($\log g < 1.75$).

One might still appeal to an extremely super metal-rich population, present only in the central regions of Seyfert galaxies, to account for the large Ca II strengths. However, for metal-rich systems $EW(\text{Mg I})$ increases with metal abundance much faster than $EW(\text{Ca II})$ (Burstein *et al.* 1984; DTT89). Hence, the hypothetical super metal-rich (with respect to the nuclear regions of ellipticals) stellar population would show a much larger enhancement of the Mg I feature than that of the Ca II triplet, just opposite to what is required.

It might be argued that the Ca II triplet absorptions could originate in the cool outermost part of an accretion disc. But the fact that the line profiles are almost Gaussian in all cases and, more importantly, that the observed line widths are similar to those found in normal galactic nuclei, as will be discussed in Section 4.3, strongly suggest a stellar origin. Therefore, the most natural interpretation of the large equivalent widths of the Ca II lines found in our sample Seyfert nuclei implies the presence of young red supergiants in their central regions. A three-component model with an old stellar population, a young stellar component and a featureless continuum in varying amounts seems to be needed, although the presence of the featureless continuum is not a necessary condition in Seyfert type 2 and LINERs; young star clusters with red supergiants should show strong Ca II triplet and weak Mg I features and therefore the combination of an old stellar population and a young one seems to be capable of explaining the observations.

4.2 Luminosity profiles

Having stated the need for a young stellar component to contribute to the continuum emission in Seyfert nuclei, it is important to establish its spatial extent. Furthermore, if a featureless continuum is also present and it actually originates in a central massive black hole, it should come from an unresolved region. For a sample of Seyfert galaxies, Malkan & Filippenko (1983) find that fractions of the total light at

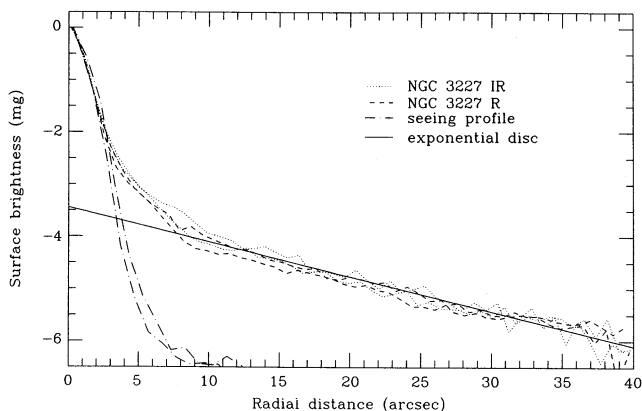


Figure 7. Radial brightness profiles from our long-slit observations of NGC 3227. Profiles at $\lambda 8500 \text{ \AA}$ (IR; dotted line) and $\lambda 6300 \text{ \AA}$ (R; broken line) are plotted, together with the seeing profile obtained from stellar observations. The solid line represents an exponential disc.

5400 \AA between 21 and 85 per cent come from an unresolved point-like source. This continuum can account for the observed dilution of the optical absorption lines. We have applied Malkan & Filippenko's methods to the Seyfert type 1 galaxy NGC 3227 for which we have obtained spectra in the region from 6200 to 9800 \AA . In Fig. 7 radial brightness profiles, as deduced from our long-slit observations, are plotted at 6300 \AA (R) and 8500 \AA (IR). Also shown is the seeing profile as deduced from stellar observations. Both profiles, the IR and the optical, are similar for the galaxy, and show a spatially unresolved nuclear component above the extrapolated disc light distribution represented by the straight line. This unresolved component effectively dominates equally the nuclear light at both wavelengths. The Mg I line is substantially diluted (see Fig. 6); yet no dilution in the Ca II lines is observed. The lack of dilution of the Ca II absorption lines in the nuclear spectra, already mentioned by Malkan & Filippenko for NGC 1068, leads naturally to the suggestion that the supposedly featureless continuum associated with the unresolved nuclear component, is not totally featureless but rather shows the presence of Ca II absorption lines, since the nuclear light is dominated by the unresolved component. According to this and our previous discussion the red supergiant stars present in the nucleus of NGC 3227 must contribute to the continuum light coming not only from the central regions but also from the unresolved source.

Spectroscopic observations with higher spatial resolution at both visual and IR wavelengths are urgently needed in order to establish definitely the different components of the continuum light of AGN.

4.3 Velocity dispersions

The central aim of this investigation was to study the IR absorption line strengths in AGN and normal galaxies. It soon became apparent, however, that the data also contained fundamental information about the velocity field in AGN.

The use of the near-IR region of the spectrum to measure the rotation and velocity dispersion in galaxies has considerable advantages with respect to the traditionally used blue-green region (Pritchet 1978; Dressler 1984b). Three aspects are particularly relevant for this work: (a) the IR is far less contaminated by both young hot stars and any blue 'featureless' continuum, traditionally postulated as the origin of the dilution of optical stellar features in the nuclear regions of AGN; (b) mismatch between the stellar template and the galaxy lines, due to different spectral type and luminosity for the template and the dominant population in the galaxy, has traditionally limited the accuracy of velocity dispersion measurements (Terlevich *et al.* 1981; Dressler 1984a). The Ca II triplet, being very strong in all but the hottest stars, considerably alleviates this problem; (c) the velocity resolution at the long wavelength of the IR Ca II triplet is twice that at the blue-optical region for the same dispersion.

These arguments suggest that our data can be used to determine accurate velocity dispersions of the stellar population in low-luminosity AGN. The importance of probing the stellar velocity field in the nuclear regions of AGN cannot be overestimated. It provides unique information about the gravitational potential close to the central engine.

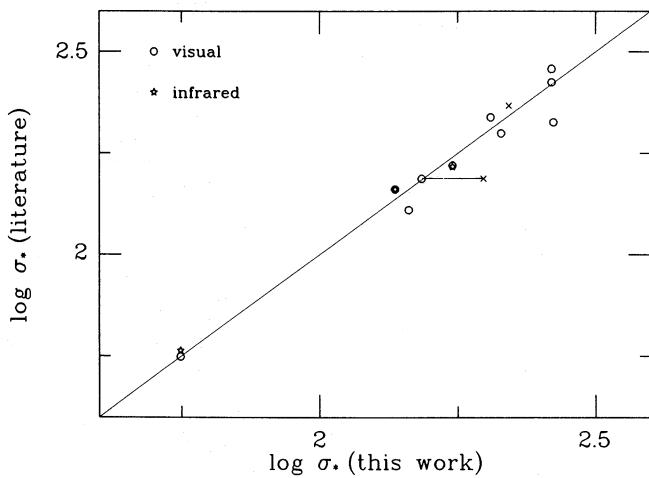


Figure 8. Velocity dispersion from this work compared with those existing in the literature (Table 5); circles and stars represent visual and infrared previous determinations, respectively. The crosses are galaxies observed with the 500-mm camera. Two observations of the same galaxy are joined together. The slope = 1 line is shown.

In this work we present the first compilation of velocity dispersions in the nuclear regions of low luminosity AGN. It includes 14 Seyfert 2 and Seyfert 1 type galaxies and 8 LINERS (see Table 3). Previous measurements exist for some of the galaxies of our sample and the comparison between our values and those found in the literature can be examined with the help of Fig. 8 where we have plotted the velocity dispersions derived in this work versus those derived by other authors for the galaxies in common as given in Table 5. The agreement is in general fairly good. The rms difference in σ is 24 km s^{-1} ; only in two of the galaxies

Table 5. Central velocity dispersions – comparison with the literature.

Galaxy	σ_{lit} & (ref.)	$\sigma_{this work}$
M 32	56 (T87)	56
	58 (DR88*)	
M 31	145 (K88)	137
	145 (DR88*)	
M 81	166 (WMcET85)	174
	165 (P78*)	
NGC 821	215 (WMcET85) 199 (G7)	213
NGC 1023	218 (WMcET85)	204
NGC 1052	212 (WMcET85)	265
NGC 1068	154 (D84)	153
		198 [†]
NGC 1700	234 (WMcET85) 233 (G7)	220 [†]
NGC 4278	243 (WMcET85)	263
NGC 4472	315 (WMcET85)	263
NGC 4736	129 (WMcET85)	145

*Infrared.

[†]500-mm camera.

References: T87: Tonry 1987; DR88: Dressler & Richstone 1988, K88: Kormendy 1988, WMcET85: Whitmore *et al.* 1985, P78: Pritchett 1978, D84: Dressler 1984b, G7: Davies *et al.* 1987.

(NGC 1052 and NGC 4472) did we find a large discrepancy. The origin of that discrepancy is not known and further work is needed. One must consider however that, for these two objects, all previous determinations of σ are based on the broadening of blue–yellow absorption features instead of IR ones. The optical part of the spectrum may be reflecting the behaviour of a different stellar mixture than the IR one. Furthermore the optical determinations are strongly affected by the presence of nuclear emission lines like H β , [O III] $\lambda\lambda 4959, 5007 \text{ \AA}$ and N I $\lambda 5200 \text{ \AA}$; this effect could be important in the case of NGC 1052.

It is interesting to see whether the stellar velocity dispersions of AGN show any systematic behaviour with respect to those of normal galaxies. Nuclear velocity dispersions of spiral galaxies are well correlated with total bulge luminosities (Whitmore, Kirshner & Schechter 1979) and furthermore, the relation between σ and L_B is essentially the same as that for elliptical galaxies (Dressler 1987). Unfortunately no light profile decomposition for our galaxies is available. We have derived bulge luminosities, therefore, by using the statistical method described by Simien & de Vaucouleurs (1986). From the total integrated magnitude listed in the *Shapley-Ames Catalog* (Sandage & Tammann 1981) the disc contribution was removed by using the relationship between the total minus bulge luminosity versus morphological type. This method should produce bulge absolute magnitudes with rms errors of about 0.5 mag.

Fig. 9 shows the measured velocity dispersion versus the derived bulge luminosity for the sample galaxies for which absolute luminosity data exist. Filled circles represent normal galaxies and LINERS while filled stars correspond to Seyfert galaxies. Also plotted in the figure are the data corresponding to elliptical galaxies (Davies *et al.* 1987, crosses) and normal spirals (Whitmore *et al.* 1979, open circles). It can be seen from the figure that the points for the Seyfert galaxies show no systematic deviation from the relation that exists for normal galaxies. The scatter in the relationship is large but it is mainly due to the fact that normal galaxies are a biparametric family and the luminosity (or effective radius) depends on both nuclear velocity dispersion and

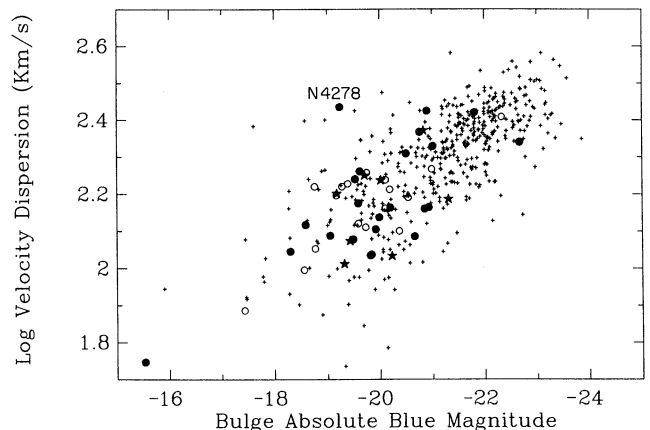


Figure 9. Measured velocity dispersion versus derived bulge luminosity. Filled circles: normal galaxies and LINERS; filled stars: Seyfert galaxies. Elliptical galaxies (Davies *et al.* 1987; crosses) and normal spirals (Whitmore *et al.* 1979; open circles) are also shown.

surface brightness (Dressler *et al.* 1987). The apparently deviant point corresponding to NGC 4278 in our sample is in fact in excellent agreement with the Davies *et al.* (1987) value for the same galaxy, which is the cross immediately to the right. It is of major importance to perform surface photometry and profile decomposition of AGN to enhance the sensitivity of the L versus σ relationship and further probe for any systematic differences between AGN and normal galaxies.

The relationship between stellar and gas velocity dispersions in AGN is another interesting point to investigate. Wilson & Heckman (1985) reported a good correlation between stellar velocity dispersions and $[\text{O III}] \lambda 5007 \text{ \AA}$ linewidths for a sample of Seyfert galaxies and LINERs with published data. The relationship showed considerable scatter but that was partially due to observational errors and lack of homogeneity of the sample. We have measured the width of the $[\text{S III}] \lambda 9069 \text{ \AA}$ line for the Seyfert galaxies in our sample by fitting a Gaussian to the core of the line. The results are given in Table 6 together with the corresponding widths of the $[\text{O III}] \lambda 5007 \text{ \AA}$ given by Dahari & De Robertis (1988) ($\sigma = 0.43$ FWHM). The comparison between stellar and gas velocity dispersions is shown in Fig. 10. Filled circles refer to $[\text{S III}]$ widths while crosses refer to $[\text{O III}]$ widths. Values corresponding to the same galaxy are connected. Arrows refer to unresolved values of $\sigma([\text{S III}])$. Contrary to Wilson & Heckman (1985), we find that only some of the sample galaxies, but including all of the Seyfert type 1s, have gas velocity dispersions which are similar to the stellar ones. There is a subset of galaxies, all Seyfert type 2 and the LINER NGC 1052, for which the emission linewidths are significantly larger than those of the absorption lines. There is no reason *a priori* for the gas and stars to sample the same potential; nevertheless there is a significant fraction of galaxies for which this is happening. The only objects which have emission lines substantially narrower than absorption lines (four arrows in the figure) are starburst galaxies. In these cases we might be detecting individual H II regions. It is

Table 6. Comparison between gas and stellar velocity dispersions.

<i>Galaxy</i>	σ_*	$\sigma([\text{SIII}])$	$\sigma([\text{OIII}])$
Mk 348	185	121	155
NGC 1052	265	372	357
NGC 1068	153	304	546
IIIZw55	212	265	—
IC342	77	*	—
Mk3	248	366	380
Mk78	115	401	286
NGC 2992	108	108	55
NGC 3227	159	235	216
NGC 3310	111	*	67
NGC 3516	235	—	104
NGC 3642	109	*	—
Mk176	149	—	206
NGC 4151	178	146	193
NGC 4388	119	108	97
NGC 5953	94	88	—
NGC 6217	131	*	—

*Unresolved.

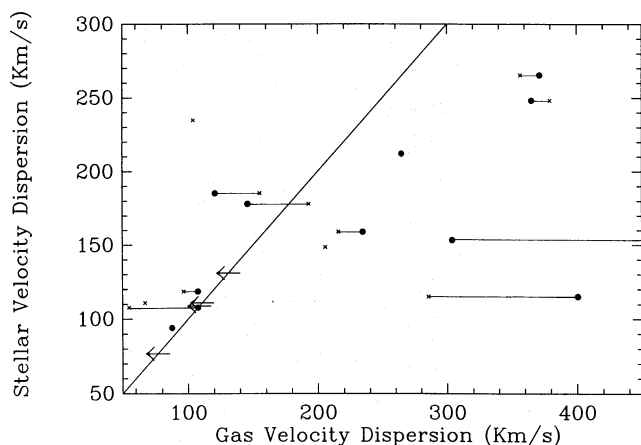


Figure 10. Stellar versus gas velocity dispersions. $[\text{S III}]$ widths are represented by filled circles and $[\text{O III}]$ ones by crosses. Unresolved values for $\sigma([\text{S III}])$ are indicated by arrows. The slope = 1 line is also drawn.

important to extend this comparison to more nuclei in order to investigate the behaviour of the excess gas broadening with AGN type.

5 Conclusions

Near-IR CCD spectroscopy for the central region of 42 AGN and normal galaxies is reported in this paper.

From the analysis of the Ca II triplet ($\lambda\lambda 8498, 8542, 8662 \text{ \AA}$) we found that in normal galaxies the distribution of the $\text{EW}(\text{Ca II})$ is very narrow with mean value 7.1 \AA and rms 0.8 \AA . Considering the wide range in luminosities, central velocity dispersions and Hubble types covered by the sample, this result is very remarkable; it is nevertheless expected if, as found by DTT89, the $\text{EW}(\text{Ca II})$ in late-type stars depends only on gravity for metallicities higher than $1/2$ solar.

The lack of correlation between σ and the strength of the IR Ca II triplet shown in Fig. 4 is also expected. The σ versus Mg_2 relationship from Terlevich *et al.* (1981) is usually interpreted, as its kindred one luminosity versus colour, in terms of mass versus metallicity. IR Ca II and σ should not be correlated in the way Mg_2 and σ are, because the IR Ca II triplet does not depend on metallicity for the abundances present in galactic nuclei (DTT89).

The IR Ca II triplet provides also new important information regarding two intrinsic properties of AGN:

- (i) the source of the nuclear light and
- (ii) the kinematics of the stars in the nuclear region.

All the Seyfert type 2 galaxies in our sample and even some Seyfert type 1, show a Ca II triplet whose strength is comparable to, and in some cases larger than, in normal galaxies. The optical stellar features in the same nuclei, however, show substantial dilution, implying that the optical-IR continuum of Seyfert galaxies *cannot* be just a combination of an old stellar component and a featureless continuum. Our results suggest the presence of an extremely young component in the nuclear stellar population of Seyfert galaxies. Super metal-rich scenarios seem ruled out by the data, but our conclusion relies on relatively inaccurate determinations of the strength of the optical Mg_2 index from the literature.

We conclude that the simplest interpretation of our results is that the large equivalent widths of the Ca II lines found in our sample Seyfert nuclei imply the presence of young red supergiants in their central regions, dominating the unresolved nuclear light at near-infrared wavelengths. A three-component model with an old stellar population, a young stellar component and a featureless continuum in varying amounts seems to be needed, although the presence of the featureless continuum is not necessary in Seyfert type 2 and LINERs; young star clusters with red supergiants should show strong Ca II triplet and weak Mg I features and therefore the combination of both an old stellar population and a young one seems to be capable of explaining the observations.

We also find that the strong IR Ca II features in Seyfert nuclei provide a unique method of probing the gravitational potential close to the central engine. This method is extremely insensitive to the presence of strong emission lines from ionized gas. We failed to find systematic deviations in the Faber-Jackson relation L_B versus σ between 'normal' and 'active' galaxies, indicating that there is no obvious excess of broadening in the stellar features of the nuclear regions of Seyfert galaxies and LINERs. Further work is needed to include the behaviour of the second parameter (surface brightness) and to improve the discrimination of the method by observing radial gradients in order to find if there is any central peak in σ , as observed in M 31 and M 32 (Dressler & Richstone 1988; Kormendy 1988).

Only a subset including the Seyfert type 1 nuclei seems to show a good correlation between the widths of the [O III] and [S III] forbidden lines and the stellar velocity dispersions, contrary to previous claims. Seyfert type 2 galaxies and the LINER NGC 1052 show an additional broadening mechanism affecting the forbidden lines, which is not seen either in the starbursts or in the Seyfert type 1 sample nuclei. It is of major interest to extend this analysis to a larger sample to see if the excess broadening is associated with other properties of Seyfert nuclei, like the radio-morphology or luminosity.

ACKNOWLEDGMENTS

The INT is operated in the island of La Palma by the RGO at the Observatorio del Roque de los Muchachos of the Instituto de Astrofísica de Canarias. We thank PATT for awarding observing time and the warm hospitality of RGO both during the realization of this work and the writing of the paper. Bernard Pagel and Michael Penston with their helpful comments greatly improved an earlier version of this paper. Collaborative grants awarded by NATO and the British Council are acknowledged.

REFERENCES

- Adams, T. F. & Weedman, D. W., 1975. *Astrophys. J.*, **199**, 19.
 Armandroff, T. E. & Zinn, R., 1988. *Astr. J.*, **96**, 92.
 Bica, E. & Alloin, D. M., 1987. *Astr. Astrophys.*, **186**, 49.
 Burstein, D., Faber, S. M., Gaskell, C. M. & Krumm, N., 1984. *Astrophys. J.*, **287**, 586.
 Carter, D., Visvanathan, N. & Pickles, A. J., 1986. *Astrophys. J.*, **311**, 637.
 Cohen, J. G., 1978. *Astrophys. J.*, **221**, 788.
 Cohen, J. G., 1979. *Astrophys. J.*, **228**, 405.
 Condon, J. J., Condon, M. A., Gisler, G. & Puschell, J. J., 1982. *Astrophys. J.*, **252**, 102.
 Dahari, D. & De Robertis, M. M., 1988. *Astrophys. J.*, **331**, 727.
 Davies, R. L., Burstein, D., Dressler, A., Faber, S. M., Lynden-Bell, D., Terlevich, R. & Wegner, G., 1987. *Astrophys. J. Suppl. Ser.*, **64**, 581.
 de Vaucouleurs, G., de Vaucouleurs, A., Corwin, H. G., Jr., 1976. *Second Reference Catalogue of Bright Galaxies*, Texas University Press, Texas.
 Díaz, A. I., Pagel, B. E. J. & Wilson, I. R. G., 1985. *Mon. Not. R. astr. Soc.*, **212**, 737.
 Díaz, A. I., Terlevich, E. & Terlevich, R., 1989. *Mon. Not. R. astr. Soc.*, **239**, 325.
 Dressler, A., 1984a. *Astrophys. J.*, **281**, 512.
 Dressler, A., 1984b. *Astrophys. J.*, **286**, 97.
 Dressler, A., 1987. *Astrophys. J.*, **317**, 1.
 Dressler, A. & Richstone, D. O., 1988. *Astrophys. J.*, **324**, 701.
 Dressler, A., Lynden-Bell, D., Burstein, D., Davies, R. L., Faber, S. M., Terlevich, R. & Wegner, G., 1987. *Astrophys. J.*, **313**, 42.
 Filippenko, A. V., 1989. *Astr. J.*, **97**, 726.
 Harwit, M. & Pacini, F., 1975. *Astrophys. J.*, **200**, L127.
 Heckman, T. M., 1987. *IAU Symp. No. 121, Observational Evidence for Activity in Galaxies*, p. 421, eds Khachikyan, E. Ye., Fricke, K. J. & Melnick, J., Reidel, Dordrecht.
 Jones, J. E., Alloin, D. M. & Jones, B. T. J., 1984. *Astrophys. J.*, **283**, 457.
 Keel, W. C., 1983. *Astrophys. J.*, **269**, 466.
 Kinman, T. D. & Davidson, K., 1981. *Astrophys. J.*, **243**, 127.
 Kormendy, J., 1988. *Astrophys. J.*, **325**, 128.
 Lawrence, A., Ward, M., Elvis, M., Fabbiano, G., Carleton, N. & Longmore, A., 1984. *Astrophys. J.*, **291**, 117.
 Malkan, M. A. & Filippenko, A. V., 1983. *Astrophys. J.*, **275**, 477.
 Melnick, J., Moles, M. & Terlevich, R., 1985. *Astr. Astrophys.*, **149**, L24.
 Morris, S. L. & Ward, M. J., 1988. *Mon. Not. R. astr. Soc.*, **230**, 639.
 Osterbrock, D. E., 1978. *Phys. Scripta*, **17**, 285.
 Pagel, B. E. J. & Edmunds, M. G., 1981. *Ann. Rev. Astr. Astrophys.*, **19**, 77.
 Phillips, M. M., Charles, P. A. & Baldwin, J. A., 1983. *Astrophys. J.*, **266**, 485.
 Phillips, M. M., Pagel, B. E. J., Edmunds, M. G. & Díaz, A. I., 1984. *Mon. Not. R. astr. Soc.*, **210**, 701.
 Pritchet, C., 1978. *Astrophys. J.*, **221**, 507.
 Pronik, I. I., 1973. *Soviet astr.*, **16**, 628.
 Rayo, J. F., Peimbert, M. & Torres-Peimbert, S., 1982. *Astrophys. J.*, **255**, 1.
 Rees, M. J., 1984. *Ann. Rev. Astr. Astrophys.*, **22**, 471.
 Rich, R. M., 1988. *Astr. J.*, **95**, 828.
 Rieke, G. H. & Lebofsky, M. J., 1979. *Ann. Rev. Astr. Astrophys.*, **17**, 477.
 Sandage, A. & Tammann, G. A., 1981. *Revised Shapley-Ames Catalog of Bright Galaxies*, Carnegie Institution of Washington, Washington DC.
 Simien, F. & de Vaucouleurs, G., 1986. *Astrophys. J.*, **302**, 564.
 Terlevich, R. & Melnick, J., 1985. *Mon. Not. R. astr. Soc.*, **213**, 841.
 Terlevich, R. & Melnick, J., 1987. In *Starbursts and Galaxy Evolution*, p. 393, eds Thuan, T. X., Montmerle, T. & Tran Thanh Van, J., Editions Frontières, Gif sur Yvette.
 Terlevich, R. & Melnick, J., 1988. *Nature*, **333**, 239.
 Terlevich, R., Melnick, J. & Moles, M., 1987. *IAU Symp. No. 121, Observational Evidence for activity in Galaxies*, p. 499, eds Khachikyan, E. Ye., Fricke, K. J. & Melnick, J., Reidel, Dordrecht.
 Terlevich, R., Davies, R. L., Faber, S. M. & Burstein, D., 1981. *Mon. Not. R. astr. Soc.*, **196**, 381.
 Tonry, J. L., 1987. *Astrophys. J.*, **322**, 632.
 Tonry, J. L. & Davis, M., 1979. *Astr. J.*, **84**, 1511.

Weedman, D. W., 1983. *Astrophys. J.*, **266**, 479.

Whitmore, B. C., Kirshner, R. P. & Schechter, P. L., 1979. *Astrophys. J.*, **234**, 68.

Whitmore, B. C., McElroy, D. B. & Tonry, J. L., 1985. *Astrophys. J. Suppl. Ser.*, **59**, 1.

Wilson, A. S. & Heckman, T. M., 1985. In: *Astrophysics of Active Galaxies and Quasi-stellar Objects*, p. 39, ed. Miller, J. S., University Science Books, Mill Valley, California.

Yee, H. K. C., 1983. *Astrophys. J.*, **272**, 473.